Threat Assessment Using Context-Based Tracking in a Maritime Environment

Jemin George
Graduate Student
jgeorge3@buffalo.edu

John L. Crassidis
Professor
johnc@buffalo.edu

Tarunraj Singh
Professor
tsingh@buffalo.edu

Department of Mechanical & Aerospace Engineering
University at Buffalo, State University of New York, Amherst, NY 14260–4400

Abstract – *The main objective of this work is to model and exploit available maritime contextual information to provide a hypothesis on suspicious vessel maneuvers. This concept involves utilizing the L1 tracking to perform L2/L3 data fusion, i.e. refinement and assessment for situations and threats. A new context-based tracker known as the ConTracker is developed. The purpose of the ConTracker is to incorporate the contextual information into a traditional $\alpha - \beta$ tracker in such a way so that it provides a repeller or an attractor characteristics to a specific region of interest. Any behavior of the vessel that is inconsistent with the repeller or the attractor characteristics of the current vessel location would be classified as suspicious. Such an inconsistent vessel behavior would be directly indicated by a high measurement residual which may be used to estimate an accurate process noise covariance using a multiple-model adaptive estimator. Based on the rate of change of the estimated process noise covariance values, an L2/L3 hypothesis generator red-flags the target vessel. Simulation results indicate that the context based tracking enhances the reliability of erratic maneuver detection.*

Keywords: Trafficability, ConTracker, MMAE, L2/L3 fusion, $\alpha - \beta$ tracker.

1 Introduction

Traditional tracking algorithms heavily rely on target model and observations but do not exploit local information. Though these approaches work well for some targets, they often fail to account for the movements of intelligent objects. Advancement of complex tracking schemes suggest that increasing the amount of information included in the algorithm can improve the quality of the tracking process. A terrain-based tracking approach which accounts for the effects of terrain on target speed and direction of movement is presented in Ref. [1]. It has been shown that the incorporation of local contextual information such as the terrain data can significantly improve the tracker performance [2]. In recent years, researchers have explored the overt use of contextual information for improving state estimation in ground target tracking by incorporating this information into the tracking algorithm as a potential field to provide a repeller or an attractor characteristic to a specific region of interest [3]. In Ref. [4], the local contextual information, termed trafficability, incorporates local terrain slope, ground vegetation and other factors to put constraints on the vehicle's maximum velocity. Simulation results given in Ref. [4] show that the use of trafficability can improve estimate accuracy in locations where the vehicle path is influenced by terrain features.

The main goal of this work is to exploit available maritime information to provide a hypothesis on suspicious boat movements. For example, it is desired to "red-flag" a boat that approaches a restricted high value unit area. Also, a vessel that is erratically zigzagging across a marked shipping channel may also be red-flagged for suspicious activity. The process to provide a hypothesis of this notion is depicted in Fig. 1. This concept involves exploiting the mathematical rigorous approaches of L1 tracking in an L2/L3 situation and threat refinement and assessment scheme (see Ref. [5] for Joint Directors of Laboratories' description of the various data fusion levels). The proposed methodology consists of three main components; a context-based tracker called ConTracker, a Multiple Model Adaptive Estimator (MMAE), and a hypothesis generator.

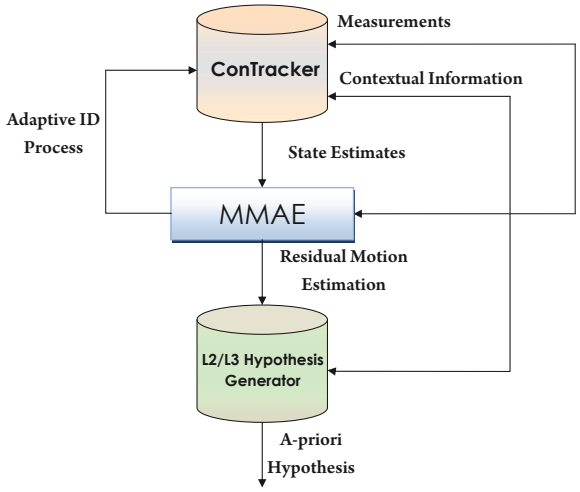

Figure 1: System Flowchart

The ConTracker (for Context-based Tracker) combines

contextual information, such as the depth, marked shipping channel locations and high value unit information, with L1 measurement information to provide state estimates (position and velocity). The purpose of the ConTracker is to use the contextual information in such a way to provide a repeller or an attractor characteristic to a specific region, developed through a grid-spaced map of a particular area of interest [3]. Any behavior of the vessel that is inconsistent with the repeller or the attractor characteristic of the current location would be classified as suspicious. Such an inconsistent vessel behavior would be directly indicated by a high measurement residual which may be used to estimate an accurate process noise covariance.

The ConTracker accuracy is not only a function of the contextual information provided, its performance also depends on the usual Kalman "tuning" issue, i.e. determination of the process noise covariance [6]. The tuning process is a function of the actual vessel motion, which can vary. This variation is the key to the hypothesis generator. This is best explained by example. Suppose that a boat is heading towards a high value unit. The contextual information incorporated into the ConTracker would repel the boat away from the high value unit during the propagation stage of the tracker. However, if the boat still proceeds towards the high value unit, which is shown directly through the measurements of the boat location, then in order to provide good tracker characteristics a high value for the process noise covariance must be chosen, i.e. tuned.

The aforementioned tuning issue is usually done in an ad-hoc manner. However, mathematical tools can be used to automatically tune the tracker. MMAE approaches are useful for process noise identification (tuning) problem. MMAE approaches run parallel trackers, each using a different value for the process noise covariance. The covariance is identified using the likelihood function of the measurement residuals, which provides weights on each individual tracker [7]. The ConTracker provides state estimates to the MMAE algorithm, which identifies the process noise covariance. This process noise covariance is fed back into the ConTracker for better tracker performance. This covariance is also incorporated into an L2/L3 hypothesis scheme that provides a hypothesis on whether or not a boat motion should be alerted to an analyst. The L2/L3 hypothesis generator "red-flags" the boat based on the rate of change of the process noise covariance and the contextual information provided. Details of these processes are provided in the proceeding sections.

2 ConTracker

The main difference between a traditional tracker and the context-based tracker is that the target model used in the ConTracker accounts for the local contextual information. The local contextual information is incorporated into the ConTracker model as trafficability values. Trafficability is a value between zero and one, where zero indicates a region that is not traversable and one indicate a region that is completely traversable. These trafficability values are based on local maritime traversability information and accounts for the following four "contextual" data:

- Depth information
- Marked channel information
- Anti-Shipping Reports (ASR)
- Locations of High-Value Units (HVU)

The individual trafficability values corresponding to each piece of contextual information is combined into a single value which would be used to indicate the repeller or the attractor characteristic of a specific region. Details of this procedure are given next.

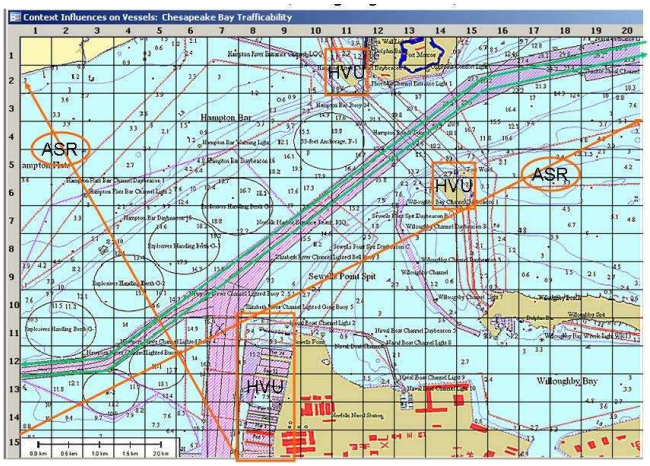

Figure 2: Maritime Trafficability Values Database

First, a particular area of interest is divided into a grid-field, similar to a 15×20 grid-field shown in Fig. 2. In Fig. 2, the purple channels indicate marked shipping lanes. As shown in Fig. 2, the area of interest contains three high-value units centered around cells $(2, 11)$, $(6, 14)$, and $(11 \ldots 15, 8)$. The area also contains two anti-shipping areas centered about cells $(4, 2)$ and $(5, 17)$. Finally, low depth areas are indicated using different shades of brown. According to the vessel type that is being tracked, a single trafficability value, ν_i, is assigned to each cell. This variable is a decimal value between 0 and 1 and corresponds to the fraction of maximum velocity that the vessel can attain in that grid location. For example, the grid cell $(10, 17)$ has a trafficability of zero due to the depth information and therefore the vessels are supposed to avoid and navigate around this particular cell.

Trafficability data will be used to deflect the direction of target motion given by the past state information. In order to implement this, at each propagation stage in the ConTracker, we consider a 3×3 trafficability grid-field that depends on the current vessel position. For example, if the vessel is located in cell $(13, 3)$, the 3×3 trafficability

grid-field consists of cells $(12,2),(12,3),(12,4),(13,2)$, $(13,3),(13,4),(14,2),(14,3)$, and $(14,4)$. A generic representation of the 3×3 trafficability grid-field is shown in Fig. 3. The vessel is assumed to be located in square 5 of the 3×3 grid. The 3×3 grid will be continually re-centered about the vessel as it moves throughout the region so that it is always located in the center (square 5) of the 3×3 trafficability grid-field. In Fig. 3, the unit vector $\hat{\mathbf{G}}_{tg} \in \mathbb{R}^2$ represents the preferred direction of the vessel strictly based on the trafficability information of the surrounding cells, $\hat{\mathbf{G}}^- \in \mathbb{R}^2$ is a unit vector in the direction of target motion given by the past state information, and the unit vector $\hat{\mathbf{G}}^+ \in \mathbb{R}^2$ represents the nudged velocity direction. A

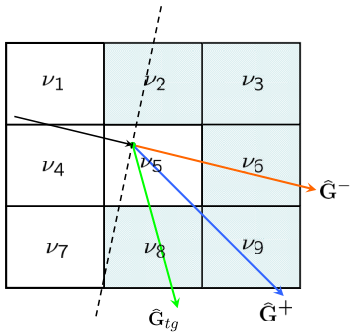

Figure 3: 3×3 Trafficability Grid-Field

preferred direction based on the velocity constraint will be calculated based upon the equation

$$\hat{\mathbf{G}}_{tg} = \frac{\sum_j (\nu_j \hat{\mathbf{G}}_j)}{\| \sum_j (\nu_j \hat{\mathbf{G}}_j) \|} \tag{1}$$

where $j \in J$ is a set of feasible directions. The unit vector $\hat{\mathbf{G}}_j \in \mathbb{R}^2$ points from the current vessel location to the center of square j. It is assumed that a vessel's velocity would not change its direction by more than ninety degrees between two consecutive time steps. Therefore, cutoff lines perpendicular to the previous direction of motion, $\hat{\mathbf{G}}^-$, will be used to limit the motion of the vessel as shown in Fig. 3. A square is assumed to be feasible if its centroid is contained within the feasible region. For this example, in Fig. 3, squares 2, 3, 6, 8 and 9 are feasible, i.e. $J = \{2,\ 3,\ 6,\ 8,\ 9\}$. Note that the vessel is allowed to change its velocity direction by more than ninety degrees if all the feasible cells have zero trafficability. The proposed technique for determining the cutoff is chosen because it is least expensive in terms of computational requirements. The assumed direction of motion is given as

$$\hat{\mathbf{G}}^+ \quad = \quad \hat{\mathbf{G}}^- + \alpha \hat{\mathbf{G}}_{tg} \tag{2}$$

where α is a weighting coefficient that is a function of ν_j. The proposed functional form for α is based on the average difference in the trafficability values between the current location and the surrounding feasible locations, μ:

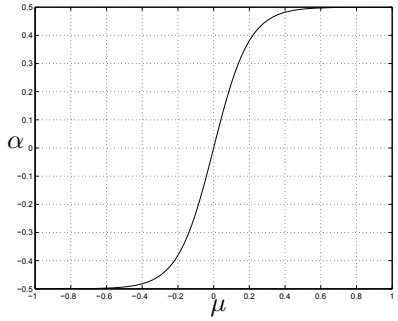

Figure 4: Proposed Form for Coefficient α

$$\mu \quad = \quad \frac{\sum_j (v_j - v_5)}{\sum_j (1)} \tag{3}$$

A plot of α versus μ is shown in Fig. 4. Since the goal is to use trafficability information to slightly alter the assumed direction, the maximum magnitude of α is chosen to be 0.5. Several cases can be discussed from this plot. First, consider the scenario where all feasible cells have the same trafficability value as the current location. When that occurs, each of the cells is equally probable and should have no influence on the overall direction. From the plot, this scenario corresponds to $\mu = 0$, which yields $\alpha = 0$. Another scenario is when the vessel is facing an impassable territory in all feasible directions (trafficability of zero). This will result in a negative μ, corresponding to a negative α. This causes the assumed direction to be directed away from the impassable regions.

2.1 Filter Algorithm

The theoretical developments of the ConTracker algorithm, which has its basis on the standard $\alpha - \beta$ tracker, are now shown. The state vector used in the filter is $\mathbf{x} \in \mathbb{R}^4$, i.e.,

$$\mathbf{x} = \begin{bmatrix} \lambda & \phi & v_\lambda & v_\phi \end{bmatrix}^T \tag{4}$$

where λ, ϕ, v_λ and v_ϕ are the longitude and latitude locations of the target vessel and the corresponding rates, respectively. The standard $\alpha - \beta$ tracker approach assumes a first-order random-walk process for the accelerations [6]. Our approach modifies this concept by using the following discrete-time model:

$$\mathbf{x}_{k+1} \quad = \quad \left[\begin{array}{c} \lambda + v_\lambda \Delta t \\ \phi + v_\phi \Delta t \\ \nu \sqrt{v_\lambda^2 + v_\phi^2} \cos\theta \\ \nu \sqrt{v_\lambda^2 + v_\phi^2} \sin\theta \end{array} \right] \Bigg|_k + \mathbf{w}_k \tag{5}$$

where

$$E\{\mathbf{w}_k \mathbf{w}_k^T\} \quad = \quad \Upsilon \begin{bmatrix} q_{1_k} & 0 \\ 0 & q_{2_k} \end{bmatrix} \Upsilon^T = \Upsilon Q_k \Upsilon^T$$

with $\Upsilon \equiv \begin{bmatrix} 0 & 0 & 1 & 0 \\ 0 & 0 & 0 & 1 \end{bmatrix}^T$. The angle θ, which is the angle between the velocity vector and the local y-axis (north axis), defines the assumed direction of motion of the vessel, $\hat{\mathbf{G}}^+$, i.e.,

$$\hat{\mathbf{G}}^+ = \begin{bmatrix} \cos\theta & \sin\theta \end{bmatrix}^T \tag{6}$$

This is determined by use of the trafficability data as explained earlier. The coefficient ν is the trafficability of the current cell. The $\sqrt{v_\lambda^2 + v_\phi^2}$ term is simply the magnitude of the vessel velocity. The trigonometric terms are used to project this value onto the appropriate axes. When no trafficability information is present, ν defaults to one, and the trigonometric terms are given by

$$\cos\theta = \frac{v_\lambda}{\sqrt{v_\lambda^2 + v_\phi^2}}, \quad \sin\theta = \frac{v_\phi}{\sqrt{v_\lambda^2 + v_\phi^2}} \tag{7}$$

which reduces to the standard $\alpha - \beta$ form. Notice that the $\hat{\mathbf{G}}^-$ in Eq. (2) is given as

$$\hat{\mathbf{G}}^- = \begin{bmatrix} \frac{v_\lambda}{\sqrt{v_\lambda^2 + v_\phi^2}} \\ \frac{v_\phi}{\sqrt{v_\lambda^2 + v_\phi^2}} \end{bmatrix} \tag{8}$$

The measurement vector is assumed to be

$$\mathbf{y} = \begin{bmatrix} \lambda & \phi \end{bmatrix}^T + \begin{bmatrix} \mathrm{v}_\lambda & \mathrm{v}_\phi \end{bmatrix}^T \tag{9}$$

where $\mathbf{v} = \begin{bmatrix} \mathrm{v}_\lambda & \mathrm{v}_\phi \end{bmatrix}^T$ is the zero mean Gaussian white-noise processes, i.e., $E[\mathbf{v}_j \mathbf{v}_k^T] = R\delta_{jk}$. Let $H = \begin{bmatrix} 1 & 0 & 0 & 0 \\ 0 & 1 & 0 & 0 \end{bmatrix}$, then $\mathbf{y} = H\mathbf{x} + \mathbf{v}$. The target model without the velocity nudging can be written in concise form as

$$\mathbf{x}_{k+1} = \Psi \mathbf{x}_k + \mathbf{w}_k \tag{10}$$

where

$$\Psi = \begin{bmatrix} 1 & 0 & \Delta t & 0 \\ 0 & 1 & 0 & \Delta t \\ 0 & 0 & 0 & 0 \\ 0 & 0 & 0 & 0 \end{bmatrix}$$

Notice that the velocity nudging is not accounted for in the filter design. The estimation error covariance is defined as $P_k = E[(\mathbf{x}_k - \hat{\mathbf{x}}_k)(\mathbf{x}_k - \hat{\mathbf{x}}_k)^T]$, and the following equations are used to propagate and update the error covariance matrix:

$$P_{k+1}^- = \Psi P_k^+ \Psi^T + \Upsilon Q_k \Upsilon^T \tag{11}$$

$$P_k^+ = [I - K_k H_k] P_k^- \tag{12}$$

where $P_k^- = E[(\mathbf{x}_k - \hat{\mathbf{x}}_k^-)(\mathbf{x}_k - \hat{\mathbf{x}}_k^-)^T]$ is the *a-priori* error covariance and $P_k^+ = E[(\mathbf{x}_k - \hat{\mathbf{x}}_k^+)(\mathbf{x}_k - \hat{\mathbf{x}}_k^+)^T]$ is the *posteriori* error covariance. The matrix K_k is the Kalman gain and can be calculated using the following equation:

$$K_k = P_k^- H^T [H P_k^- H^T + R]^{-1} \tag{13}$$

The vector $\hat{\mathbf{x}}_k^-$ is referred to as the *a-priori* state estimate and the vector $\hat{\mathbf{x}}_k^+$ is referred to as the *posteriori* state estimate. The estimates are propagated and updated using the following equations:

$$\hat{\mathbf{x}}_{k+1}^- = \left[\begin{array}{c} \hat{\lambda}^+ + \hat{v}_\lambda^+ \Delta t \\ \hat{\phi}^+ + \hat{v}_\phi^+ \Delta t \\ \nu \sqrt{(\hat{v}_\lambda^+)^2 + (\hat{v}_\phi^+)^2} \cos\theta \\ \nu \sqrt{(\hat{v}_\lambda^+)^2 + (\hat{v}_\phi^+)^2} \sin\theta \end{array} \right]_k \tag{14}$$

$$\mathbf{x}_k^+ = \mathbf{x}_k^- + K_k[\mathbf{y}_k - H\mathbf{x}_k^-] \tag{15}$$

The ConTracker algorithm is summarized in Table 1. Note that the process noise covariance Q_k is indicative of how accurate the target model is. If the target vessel follows the model precisely, then Q_k would be fairly small. If the vessel maneuvers are erratic and inconsistent with the model, then the process noise covariance would be large. Since we do not know the precise value of the process noise covariance, an MMAE is implemented to estimate the process noise covariance based on the measurement residual.

Table 1: Summary of ConTracker Algorithm

Initialize
$\hat{\mathbf{x}}(t_0) = \hat{\mathbf{x}}_0^-, P_0^- = E[(\mathbf{x}_0 - \hat{\mathbf{x}}_0^-)(\mathbf{x}_0 - \hat{\mathbf{x}}_0^-)^T]$
Kalman Gain
$K_k = P_k^- H^T [H P_k^- H^T + R]^{-1}$
Update
$\hat{\mathbf{x}}_k^+ = \hat{\mathbf{x}}_k^- + K_k[\mathbf{y}_k - H\hat{\mathbf{x}}_k^-]$
$P_k^+ = [I - K_k H_k] P_k^-$
Velocity Nudging
$\hat{\mathbf{G}}^- = \left[\begin{array}{c} \frac{\hat{v}_\lambda^+}{\sqrt{(\hat{v}_\lambda^+)^2 + (\hat{v}_\phi^+)^2}} \\ \frac{\hat{v}_\phi^+}{\sqrt{(\hat{v}_\lambda^+)^2 + (\hat{v}_\phi^+)^2}} \end{array} \right]_k, \hat{\mathbf{G}}_{tg} = \frac{\sum_j (\nu_j \hat{\mathbf{G}}_j)}{\| \sum_j (\nu_j \hat{\mathbf{G}}_j) \|}$
$\hat{\mathbf{G}}^+ = \hat{\mathbf{G}}^- + \alpha \hat{\mathbf{G}}_{tg}$
$\begin{bmatrix} \cos\theta & \sin\theta \end{bmatrix}^T = \hat{\mathbf{G}}^+$
Propagation
$P_{k+1}^- = \Psi P_k^+ \Psi^T + \Upsilon Q_k \Upsilon^T$
$\hat{\mathbf{x}}_{k+1}^- = \left[\begin{array}{c} \hat{\lambda}^+ + \hat{v}_\lambda^+ \Delta t \\ \hat{\phi}^+ + \hat{v}_\phi^+ \Delta t \\ \nu \sqrt{(\hat{v}_\lambda^+)^2 + (\hat{v}_\phi^+)^2} \cos\theta \\ \nu \sqrt{(\hat{v}_\lambda^+)^2 + (\hat{v}_\phi^+)^2} \sin\theta \end{array} \right]_k$

3 MMAE

In this section a brief overview of the MMAE approach is shown. More details can be found in Refs. [7–9]. Multiple-model adaptive estimation is a recursive estimator that uses a bank of filters that depend on some unknown parameters. In our case these parameters are the process noise variances (diagonal elements of the process noise covariance), denoted by the vector $\mathbf{q}_k = \begin{bmatrix} q_{1_k} & q_{2_k} \end{bmatrix}$. For notational simplicity the subscript k is omitted for $\mathbf{q}$. Initially a set of distributed elements is generated from some known probability density function (pdf) of $\mathbf{q}$, denoted by $p(\mathbf{q})$, to give $\{\mathbf{q}^{(\ell)};\, \ell = 1, \ldots, M\}$. Here M denotes the number of filters in the filter bank. The goal of the estimation process is to determine the conditional pdf of the ℓ^{th} element $\mathbf{q}^{(\ell)}$ given the current-time measurement $\mathbf{y}_k$. Application of Bayes' Law yields

$$p(\mathbf{q}^{(\ell)}|\mathbf{Y}_k) = \frac{p(\mathbf{Y}_k, \mathbf{q}^{(\ell)})}{p(\mathbf{Y}_k)} = \frac{p(\mathbf{Y}_k|\mathbf{q}^{(\ell)})\, p(\mathbf{q}^{(\ell)})}{\sum_{j=1}^{M} p(\mathbf{Y}_k|\mathbf{q}^{(j)})\, p(\mathbf{q}^{(j)})} \quad (16)$$

where $\mathbf{Y}_k$ denotes the sequence $\{\mathbf{y}_0, \mathbf{y}_1, \ldots, \mathbf{y}_k\}$. The probabilities $p(\mathbf{q}^{(\ell)}|\mathbf{Y}_k)$ can be computed through [7]

$$\begin{aligned} p(\mathbf{q}^{(\ell)}|\mathbf{Y}_k) &= \frac{p(\mathbf{y}_k, \mathbf{Y}_{k-1}, \mathbf{q}^{(\ell)})}{p(\mathbf{y}_k, \mathbf{Y}_{k-1})} \\ &= \frac{p(\mathbf{y}_k|\mathbf{Y}_{k-1}, \mathbf{q}^{(\ell)})\, p(\mathbf{q}^{(\ell)}|\mathbf{Y}_{k-1}) p(\mathbf{Y}_{k-1})}{p(\mathbf{y}_k|\mathbf{Y}_{k-1}) p(\mathbf{Y}_{k-1})} \\ &= \frac{p(\mathbf{y}_k|\hat{\mathbf{x}}_k^{-(\ell)})\, p(\mathbf{q}^{(\ell)}|\mathbf{Y}_{k-1})}{\sum_{j=1}^{M} \left[p(\mathbf{y}_k|\hat{\mathbf{x}}_k^{-(j)})\, p(\mathbf{q}^{(j)}|\mathbf{Y}_{k-1}) \right]} \end{aligned}$$

since $p(\mathbf{y}_k, |\mathbf{Y}_{k-1}, \mathbf{q}^{(\ell)})$ is given by $p(\mathbf{y}_k|\hat{\mathbf{x}}_k^{-(\ell)})$ in the Kalman recursion. The recursion formula can be cast into a set of defined weights $\varpi_k^{(\ell)}$, so that

$$\varpi_k^{(\ell)} = \varpi_{k-1}^{(\ell)} p(\mathbf{y}_k|\hat{\mathbf{x}}_k^{-(\ell)}), \qquad \varpi_k^{(\ell)} \leftarrow \frac{\varpi_k^{(\ell)}}{\sum_{j=1}^{M} \varpi_k^{(j)}} \quad (17)$$

where $\varpi_k^{(\ell)} \equiv p(\mathbf{q}^{(\ell)}|\tilde{\mathbf{y}}_k)$. The weights at time t_0 are initialized to $\varpi_0^{(\ell)} = 1/M$ for $\ell = 1, 2, \ldots, M$. The convergence properties of the MMAE are shown in Ref. [7], which assumes ergodicity in the proof. The ergodicity assumptions can be relaxed to asymptotic stationarity and other assumptions are even possible for non-stationary situations [10]. The conditional mean estimate is the weighted sum of the parallel filter estimates:

$$\hat{\mathbf{x}}_k^- = \sum_{j=1}^{M} \varpi_k^{(j)} \hat{\mathbf{x}}_k^{-(j)} \quad (18)$$

Also, the error covariance of the state estimate can be computed using

$$P_k^- = \sum_{j=1}^{M} \varpi_k^{(j)} \left[\{P_k^-\}^{(j)} + \left(\hat{\mathbf{x}}_k^{-(j)} - \hat{\mathbf{x}}_k^- \right) \left(\hat{\mathbf{x}}_k^{-(j)} - \hat{\mathbf{x}}_k^- \right)^T \right] \quad (19)$$

The specific estimate for $\mathbf{q}$ at time t_k, denoted by $\hat{\mathbf{q}}_k$, and error covariance, denoted by $\mathcal{P}_k$, are given by

$$\hat{\mathbf{q}}_k = \sum_{j=1}^{M} \varpi_k^{(j)} \mathbf{q}^{(j)} \quad (20a)$$

$$\mathcal{P}_k = \sum_{j=1}^{M} \varpi_k^{(j)} \left(\mathbf{q}^{(j)} - \hat{\mathbf{q}}_k \right) \left(\mathbf{q}^{(j)} - \hat{\mathbf{q}}_k \right)^T \quad (20b)$$

Equation (20b) can be used to define 3σ bounds on the estimate $\hat{\mathbf{q}}_k$ [11]. Notice that the estimated process noise covariance from the MMAE, $Q_k = \begin{bmatrix} \hat{q}_{1_k} & 0 \\ 0 & \hat{q}_{2_k} \end{bmatrix}$, is fed back into the ConTracker and the L2/L3 hypothesis generator.

4 L2/L3 Hypothesis Generator

As mentioned earlier, the estimated process noise covariance is indicative of how well the target vessel follows the near-constant velocity model. The incorporation of trafficability data into the model allows variations in target vessel velocity that are consistent with the given contextual information. For example, if the target vessel in cell $(7, 13)$ of Fig. 2 that is traveling toward cell $(5, 15)$ makes a sharp right turn to avoid the high-value unit in cell $(6, 14)$, then the sudden change in vessel's velocity is consistent with the trafficability data provided and therefore the vessel would not be red-flagged. However, if the target vessel in cell $(6, 3)$ that is traveling toward cell $(3, 1)$ continues to travel in a straight line with a constant velocity, then the vessel would be red-flagged despite its consistent behavior in accordance with the near-constant velocity model. This is because its passage into cell $(5, 2)$ is in contrast to the anti-shipping activities reported in that area. Thus, the incorporation of the trafficability data into the near-constant velocity model assesses the reliability of L2/L3 hypothesis generator.

The near-constant velocity model combined with the trafficability information is given by

$$\mathbf{x}_{k+1} = \left[\begin{array}{c} \lambda + v_\lambda \Delta t \\ \phi + v_\phi \Delta t \\ \nu \sqrt{v_\lambda^2 + v_\phi^2} \cos\theta \\ \nu \sqrt{v_\lambda^2 + v_\phi^2} \sin\theta \end{array} \right]_k + \mathbf{w}_k \quad (21)$$

Any abrupt maneuver of the target vessel that is inconsistent with the near-constant velocity model or the trafficability information can be treated as process noise. This would in turn result in a sudden increase in the process noise covariance estimated by the MMAE. The two main objectives

of the L2/L3 hypothesis generator are to red-flag a vessel based on the anomalies in its behavior that is indicated by the change in process noise covariance and identify the reason behind the red-flagging.

In order to red-flag a target vessel, we consider two sets of process noise covariance values. One set, $\{\hat{q}_{1_k}, \quad \hat{q}_{2_k}\}$ is the MMAE estimate based on the ConTracker measurement residual values and the second set, $\{\breve{q}_{1_k}, \quad \breve{q}_{2_k}\}$ is a second pair of MMAE estimates based on a standard $\alpha-\beta$ tracker. The only difference between these two trackers is that the standard $\alpha-\beta$ tracker does not make use of any contextual information. The second set of estimates, $\{\breve{q}_{1_k}, \quad \breve{q}_{2_k}\}$, are used to normalize the first set of process noise covariance values. The normalized process noise covariances values are given as

$$\bar{q}_{1_k} = \frac{\hat{q}_{1_k}}{\breve{q}_{1_k}}, \quad \bar{q}_{2_k} = \frac{\hat{q}_{2_k}}{\breve{q}_{2_k}} \tag{22}$$

Normalization would allow to eliminate any minor deviations in the process noise covariance values due to additive measurement noise. It also helps to clearly identify any abrupt maneuver of the target vessel that is inconsistent with the given trafficability information. After normalizing the elements of the process noise covariance matrix, their Euclidian norm is calculated as $||q_k|| = \sqrt{(\bar{q}_{1_k})^2 + (\bar{q}_{2_k})^2}$. The rate of change of the normalized process noise covariance norm can be calculated as $\Delta q_k = \frac{1}{\Delta t}\left[||q_k|| - ||q_{k-1}||\right]$. Finally a vessel is red-flagged if the rate of change on the normalized process noise covariance norm is greater than a prescribed threshold, i.e. $\Delta q_k > \Delta q_{\max} \Rightarrow$ Red-Flag.

The red-flagging reasoner deals with identifying the contextual information that is conflicting with the current target vessel location. For example, the grid cell $(2, 11)$ of Fig. 2 has a trafficability of zero due to the high-value unit location. Therefore if a vessel is located in cell $(2, 11)$, then the conflicting contextual information is the high-value unit locations. Since the ConTracker is assumed to have access to all the contextual information, the simplest red-flagging reasoner can be synthesized by identifying which of the four contextual data contributes to the zero trafficability at the current location. The main assumption behind this approach is that there is only one piece of contextual information that is contributing to the zero trafficability at any specific time. A main disadvantage of this red-flagging reasoner is that if the observed target locations are highly noisy, then the estimated target location and the corresponding trafficability value may not be consistent with the true location and the true trafficability value. This problem can be resolved by considering large enough grid size and accurate measurements.

5 Results

In order to evaluate the performance of the proposed scheme, a test case scenario is developed where we consider Hampton Roads Bay, Virginia, near the Norfolk Naval Station. The area of interest is first divided into a 15×20 grid-field as shown in Fig. 2. Afterwards a trafficability value is assigned to each cell based on the target vessel type and the individual contextual data. As shown in Fig. 2, the harbor area contains three high-value units centered around cells $(2, 11)$, $(6, 14)$, and $(11 \ldots 15, 8)$. The harbor area also contains two anti-shipping areas centered about cells $(4, 2)$ and $(5, 17)$. There are several marked shipping lanes in the harbor area that are indicated by shaded purple channels.

For simulation purposes we consider two different ski boats. Both ski boat tracks are indicated by orange lines in Fig. 2. Details on the individual Ski Boats are given below.

- Ski Boat 1: Ski Boat 1 starts in cell $(15, 8)$ and travels toward cell $(2, 1)$. Ski Boat 1 crosses over two different marked channels at cells $(14, 7)$ and $(11, 5)$ while heading toward the distressed vessel. Afterwards, the Ski Boat 1 crosses over a anti-shipping area located around cell $(14, 2)$ and travels towards cell $(2, 1)$.

- Ski Boat 2: Ski Boat 2 starts in cell $(15, 1)$ and travels toward cell $(4, 20)$. Ski Boat 2 crosses over a marked channel in cell $(11, 7)$ and a high-value unit area located in cell $(11, 8)$. Ski Boat 2 crosses over a second high-value unit area located about cell $(6, 14)$ and an anti-shipping area located around cell $(5, 17)$ while traveling toward cell $(4, 20)$.

Due to constraints on space, here we only consider the simulations results for the second ski boat.

5.1 Ski Boat 2

As shown in Fig. 2, the second ski boat starts in cell $(15, 1)$ and travels toward cell $(4, 20)$. Figure 5 shows the measured, $\mathbf{y}$, and estimated, $H\hat{\mathbf{x}}$, tracks for ski boat 2. Figure 6(a) contains the estimated process noise covariance

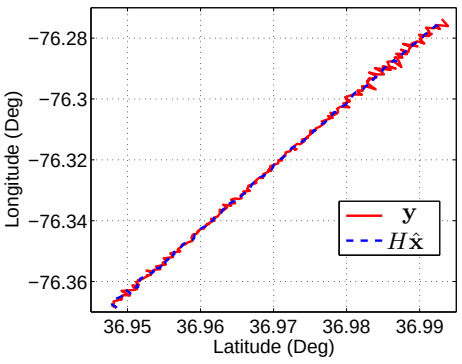

Figure 5: Ski Boat 2 Track: Measured & ConTracker Estimate

variance values from the ConTracker/MMAE $\{\hat{q}_{1_k}, \hat{q}_{2_k}\}$ and the $\alpha-\beta$ tracker/MMAE $\{\breve{q}_{1_k}, \breve{q}_{2_k}\}$. Figure 6(b) shows

the normalized process noise covariance norm, $||q_k||$, for ski boat 2. Notice the sudden increase in $||q_k||$ at times 420 sec, 490 sec, 900 sec, 970 sec and 1020 sec. The first increase in the process noise covariance values occurs when ski boat 2 crosses over the marked channel located about cell $(11, 7)$. The second increase in the process noise covariance values occurs when ski boat 2 crosses over a high-value unit area located about the cell $(11, 8)$ around 490 sec. The third jump in the process noise covariance values occurs when the ski boat enters a second high-value unit area located about cell $(6, 14)$ around 900 sec. The fourth increase in the estimated process noise covariance value occurs when the target vessel travels through a low depth area located in cell $(6, 16)$ around 970 sec. The final increase in the process noise covariance occurs when ski boat 2 enters the anti-shipping area located about cell $(5, 17)$ around 1020 sec.

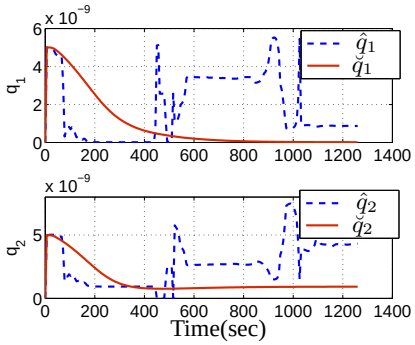

(a) Estimated q_1 and q_2

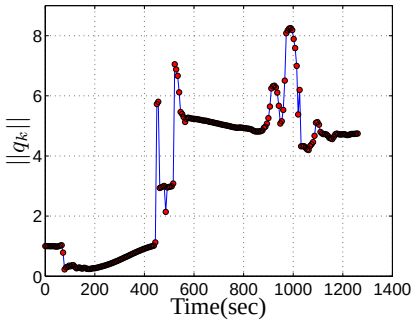

(b) Normalized Process Noise Covariance Norm

Figure 6: ConTracker & $\alpha - \beta$ Tracker Estimated Process Noise Covariance and Normalized Norm for Ski Boat 2

Shown in Fig. 7 are the rate of change of normalized process noise covariance norm, Δq_k, and the trafficability values, ν for ski boat 2. The maximum allowable Δq_k for ski boat 2 is selected to be $\Delta q_{max} = 0.30$. Notice that at times 420 sec, 490 sec, 900 sec, 970 sec and 1020 sec, Δq_k is higher than its threshold value and therefore the target vessel would be red-flagged at these instances. Also note the low trafficability values at these instances as shown in Fig 7(b).

Figure 8(a) shows the angle between the velocity vector and the local y-axis for the ConTracker and the $\alpha-\beta$ tracker.

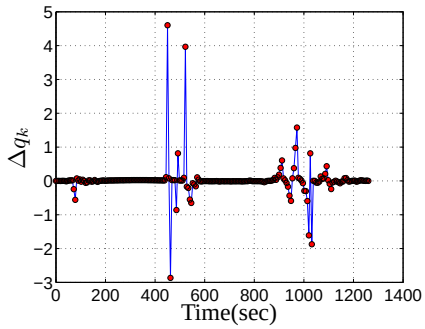

(a) Rate of Change of Normalized Process Noise Covariance Norm

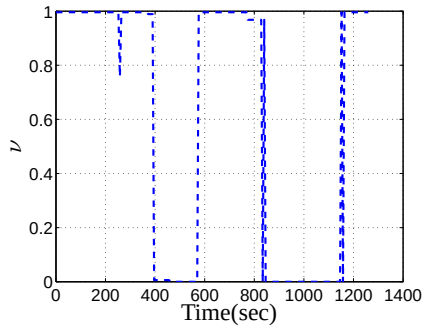

(b) Trafficability Values

Figure 7: Time History of Rate of Change of Normalized Process Noise Covariance Norm and Trafficability Values for Ski Boat 2

Notice that the angle obtained from the $\alpha - \beta$ tracker is much smoother compared to the one obtained from the ConTracker. The discrepancies in the ConTracker's angle is due to the velocity nudging that occurs when the target vessel encounters a zero-trafficability area. Figure 8(b) shows the red-flag alerts for ski boat 2. Note that the red-flag occurrence and the large deviations in θ are consistent with the results shown in Fig. 7.

6 Conclusion

The objective of this work is to model and exploit available maritime contextual information to provide a hypothesis on suspicious vessel maneuvers. This concept involves utilizing the L1 tracking approach to perform L2/L3 situation and threat, refinement and assessment. A new context based tracker known as the ConTracker is developed here. This tracker, which has its foundation in the standard $\alpha - \beta$ tracker incorporates the available contextual information into the target vessel model as trafficability values. Based on the trafficability values, the target vessel is either attracted or repelled from a particular area. Though the traditional $\alpha - \beta$ tracker uses a near-constant velocity model, the ConTracker allows reasonable variations in velocity that

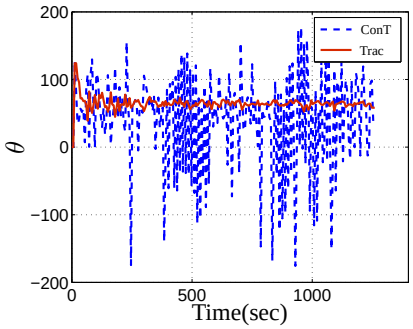

(a) Boat Direction

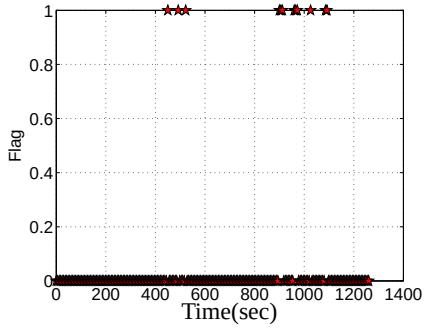

(b) Red-Flag Indicator

Figure 8: ConTracker & $\alpha - \beta$ Tracker Estimated Direction and Red-Flag Indicator for Ski Boat 2

are consistent with the contextual information. But abrupt variations in velocity (variations not due to trafficability influence) would account for erratic maneuver. The accuracy of the ConTracker estimates depends on the contextual data and the process noise covariance value, which is a tuning parameter. A multiple model adaptive estimator is implemented to estimate the accurate process noise covariance value. Variations in velocity that are inconsistent with the contextual information would result in an increase in the estimated process noise covariance value. Based on the rate of change of the estimated process noise covariance values, an L2/L3 hypothesis generator red-flags the target vessel. Simulation results indicate that the context based tracking enhances the reliability of erratic maneuver detection.

7 Acknowledgement

This work was supported by Silver Bullet Solutions through an Office of Naval Research grant. The authors wish to thank David McDaniel and Todd Kingsbury from Silver Bullet Solutions for their support and generation of data that was used in this paper.

References

[1] Reid, D. B. and Bryson, R. G., "A Non-Gaussian Filter for Tracking Targets Moving Over Terrain," *Proceedings of the 12th Annual Asilomar Conference on Circuits, Systems, and Computers*, Pacific Grove, CA, Nov. 1978, pp. 112–116.

[2] Nougues, P. O. and Brown, D. E., "We Know Where You Are Going: Tracking Objects in Terrain," *IMA Journal of Mathematics Applied in Business & Industry*, Vol. 8, 1997, pp. 39–58.

[3] Tenne, D., Pitman, B., Singh, T., and Llinas, J., "Velocity Field Based Tracking of Ground Vehicles," *RTO-SET-059: Symposium on "Target Tracking and Sensor Data Fusion for Military Observation Systems*, Budapest, Hungary, Oct. 2003.

[4] Fosbury, A. M., Singh, T., Crassidis, J. L., and Springen, C., "Ground Target Tracking Using Terrain Information," 10th *International Conference on Information Fusion*, July 2007.

[5] Kessler, O. and White, F., "Data Fusion Perspectives and Its Role in Information Processing," *Handbook of Multisensor Data Fusion: Theory and Practice*, edited by M. E. Liggins, D. L. Hall, and J. Llinas, chap. 2, CRC Press, Boca Raton, FL, 2009.

[6] Crassidis, J. L. and Junkins, J. L., *Optimal Estimation of Dynamic Systems*, CRC Press, Boca Raton, FL, 2004.

[7] Anderson, B. and Moore, J. B., *Optimal Filtering*, Dover Publications, Mineola, NY, 1979.

[8] Brown, R. G. and Hwang, P., *Introduction to Random Signals and Applied Kalman Filtering*, John Wiley & Sons, New York, NY, 3rd ed., 1997, pp. 353–361.

[9] Stengel, R. F., *Optimal Control and Estimation*, Dover Publications, New York, NY, 1994, pp. 402–407.

[10] Anderson, B., Moore, J. B., and Hawkes, R. M., "Model Approximations via Prediction Error Identification," *Automatica*, Vol. 14, No. 6, Nov. 1978, pp. 615–622.

[11] Crassidis, J. L. and Cheng, Y., "Generalized Multiple-Model Adaptive Estimation Using an Autocorrelation Approach," *Proceedings of the 9th International Conference on Information Fusion*, Florence, Italy, July 2006, paper 223.